Numerical modelling of waves in piezo-substrates: for the electromechanical characterization of acoustic wave filters

Yingzi Ying

September 30, 2022

Contents

1 Introduction

This is an interim report for the collaboration research project between Huawei and KTH. The project aims to progressively make a numerical tool that is capable to efficiently and accurately simulate acoustic wave resonators. Through the numerical simulations, we hope to reveal the intrinsic mechanism of electromechanical behaviour of acoustic wave filters, and validate filter prototyping design, quantify and optimise the geometrical and material configurations.

The acoustic wave resonators, a micro electro-acoustic devices, fall into two categories: the bulk acoustic wave resonators and the surface acoustic wave resonators, which are distinguished by different propagation modes in piezoelectric substrates[1]. The acoustic waves are excited by the applied electric field from the electrodes through the converse piezoelectric effect, and also detected on the electrodes through the direct piezoelectric effect. Piezoelectricity is a process to convert mechanical energy into electrical energy, or vice versa. The coherent superposition of the propagating waves can result resonant phenomenon thus can select signal content at particular frequency ranges.

The numerical tool should include the functional modules to simulate the excitation, propagation and detection processes of acoustic waves in piezoelectric substrates. Furthermore, the key duty is to simulate how the acoustic waves propagate in piezoelectric substrates, which are

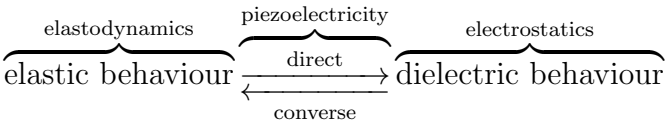

Figure 1: Schematic diagram about the numerical simulation of acoustic wave filters.

naturally anisotropic media, and the waves are governed by the linear elastodynamics. The acoustic waves in chips intrinsically mimic the earthquakes on micro scales. To act on instinct, we may resort to the methodology that is popular in the computational seismology community, in which both the theories, numerical methods and tools have been well developed, to help solving our problem in the simulation of acoustic waves in piezoelectric substrates.

Our code development is mainly based on the SPECFEM open-source packages, which are released in the 2D and 3D versions. The software packages are primarily for the simulation of seismic waves based upon the spectral-element method, which is a higher order finite-element method using the Galerkin technique that can achieve optimized efficiency and excellent accuracy. It was first developed by Dimitri Komatitsch at Institut de Physique du Globe in Paris[2], later at Harvard and Caltech together with Jeroen Tromp[3], then has been developed and maintained by a global team of scientists from top universities[4, 5, 6]. SPECFEM has become one of the most popular community code to simulate mechanical wave propagation in fluid, solid and porous media and is widely used by many seismologists and acousticians. The software is written with Fortran90 programming language and uses the Message Passing Interface for parallel programming, that is very well suited to the implementation on supercomputers to solve large scale problems. It has an internal mesher, named MESHFEM, but can also support other third-party meshing software to create arbitrarily shaped models. The software code is publish under the GNU General Public Licence that you receive source code or can get it if you want it, that you can change the software or use pieces of it in new free programs, and that you know you can do these things[7]. We use SPECFEM as the solver of acoustic wave propagation, and further customise and develop functional modules of electrostatics and piezoelectricity for the full-stack implementation of the numerical simulator of acoustic wave resonators.

In this report, we first present the fundamental theories govern the generation, propagation and receiving of acoustic waves in piezoelectric substrates, followed by an instruction to use the code. We also present simple numerical examples for illustration, and give a summary of the achieved work and look into the future work.

2 Fundamental theories

As shown in Figure 1 for the illustration about the intrinsic mechanism of acoustic wave filters, the fundamental theories guide the simulation of acoustic wave resonators consist of 3 main parts: electrostatics, piezoelectricity and elastodynamics. The electrical motions and mechanical motions are characterised by the electrostatics and elastodynamics, respectively. The piezoelectricity, both the direct and converse effects, bridges the electrical and mechanical counterparts that can convert in between the two different energy types.

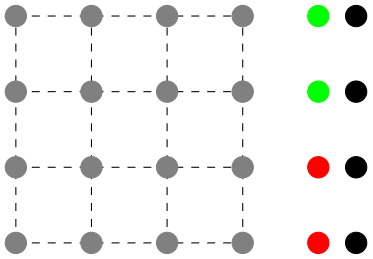

Figure 2: Illustration for the calculation method of electric filed.

2.1 Electrostatics

The acoustic wave propagates in a piezoelectric substrate much slower than the speed of electric field, that in each mechanical motion step, the electric charges are not in movement that the electric field is unchanged. So no significant magnetic field is induced that we can just use the electrostatic equations to calculate the electrical properties.

The first step in simulating the acoustic wave filters is to accurately calculate the electric field generated by the electrodes with an applied voltage signal. We propose and develop a fast algorithm for the electric field calculation. As shown in Figure 2, the positive and negative, or neutral, electrodes are depicted with the discrete red and green dots, respectively, and the black dots denote the equivalent source array in adjacent to the electrodes. The grey array dots denote the spatial points where the electric field need to be calculated.

As known from the Coulomb's law, the electric potential field at $\boldsymbol{x}_\mathrm{r}$ from a point electric charge q at point $\boldsymbol{x}_\mathrm{s}$ is

$$\phi(\boldsymbol{x}_\mathrm{r}, \boldsymbol{x}_\mathrm{s}) \begin{cases} -\frac{q}{2\pi\epsilon_0} \ln(\|\boldsymbol{x}_\mathrm{r} - \boldsymbol{x}_\mathrm{s}\|) & \text{in 2D;} \\ \frac{q}{4\pi\epsilon_0} \frac{1}{\|\boldsymbol{x}_\mathrm{r} - \boldsymbol{x}_\mathrm{s}\|} & \text{in 3D,} \end{cases} \tag{1}$$

where ϵ_0 denotes the vacuum permittivity. Assume the equivalent source array has an unknown electric charge distribution $\boldsymbol{q} = (q_n) \in \mathbb{R}^N$, which subjects to the constant electric potential on electrodes $\boldsymbol{\phi}_0 = (\phi_{0m}) \in \mathbb{R}^M$, that is

$$\boldsymbol{\phi}_0 = \boldsymbol{\Phi}\boldsymbol{q}. \tag{2}$$

The linear system $\boldsymbol{\Phi} = (\phi_{mn}) \in \mathbb{R}^{M\times N}$ is the transfer matrix with elements from the nth source point to the mth point on electrodes.

Finally, the electric potential at arbitrary spatial points $\boldsymbol{\phi} = (\phi_l) \in \mathbb{R}^L$ can be expressed with the new transfer matrix $\boldsymbol{\Phi}' = (\phi_{ln}) \in \mathbb{R}^{L\times N}$

$$\boldsymbol{\phi} = \boldsymbol{\Phi}'\boldsymbol{\Phi}\backslash\boldsymbol{\phi}_0. \tag{3}$$

From the Maxwell's Law, the electric field is the negative gradient of electric potential field, that is

$$\boldsymbol{E}(\boldsymbol{x}) = -\nabla\phi(\boldsymbol{x}). \tag{4}$$

The electric displacement field is the multiplication of the electric field and the dielectric constant, or permittivity:

$$\boldsymbol{D} = \boldsymbol{\epsilon} \cdot \boldsymbol{E}. \tag{5}$$

From the Gauss's Law, the electric charge density ρ is the divergence of electric displacement field

$$\nabla \cdot \boldsymbol{D} = \rho. \tag{6}$$

Alternatively, the total electric charge accumulated on an electrode can be obtained by integrating the electric displacement over the electrode surface

$$Q = \oint_S \boldsymbol{D} \cdot d\boldsymbol{s}. \tag{7}$$

The electric current passing through the electrode is just the time derivative of electric charge:

$$I = \frac{dQ}{dt}. \tag{8}$$

2.2 Piezoelectricity

Piezoelectricity can couple the elastic behaviour with the dielectric behaviour, and the effect is reversible. The direct piezoelectric effect is the production of electricity when a stress is applied on material, and the converse piezoelectric effect is the production of stress when an electric field is applied.

The piezoelectric constitutive relationship in a stress-charge form can be expressed as[8]:

$$\boldsymbol{\sigma} = \overset{\text{elasticity}}{\boldsymbol{c} : \boldsymbol{\varepsilon}} - \overset{\text{converse}}{\boldsymbol{e}^{\mathrm{T}} \cdot \boldsymbol{E}}, \tag{9}$$

$$\boldsymbol{D} = \overset{\text{dielectricity}}{\boldsymbol{\epsilon} \cdot \boldsymbol{E}} + \overset{\text{direct}}{\boldsymbol{e} : \boldsymbol{\varepsilon}}. \tag{10}$$

Here $\boldsymbol{e}$ is the piezoelectric coupling tensor, $\boldsymbol{\epsilon}$ is the dielectric tensor, and $\boldsymbol{c}$ is the elastic tensor.

The mathematical model of piezoelectricity consists of the mechanical equation describing elastodynamics and the electrical equation describing electrostatics. The piezoelectric material is both an elastic material and a dielectric material.

2.3 Elastodynamics

The acoustic waves in piezoelectric substrates are generally governed by the non-homogeneous linear elastodynamics

$$\rho \ddot{\boldsymbol{u}} - \nabla \cdot \boldsymbol{\sigma} = \boldsymbol{f}^{\mathrm{m}} + \boldsymbol{f}^{\mathrm{p}}, \tag{11}$$

where the stress and strain is related with the elastic constant $\boldsymbol{c}$ under the Hooke's law:

$$\boldsymbol{\sigma} = \boldsymbol{c} : \boldsymbol{\varepsilon}, \tag{12}$$

and the strain is the symmetric part of displacement gradient,

$$\boldsymbol{\varepsilon} = (\nabla \boldsymbol{u} + \nabla \boldsymbol{u}^{\mathrm{T}})/2. \tag{13}$$

In Eq. (11), we can see that the stress, or the body force as its divergence $\boldsymbol{f}^{\mathrm{p}} = \nabla \cdot (-\boldsymbol{e}^{\mathrm{T}} \cdot \boldsymbol{E})$, resulted from the converse piezoelectric effect can play the role as the vibrating sources. The external mechanical body force term $\boldsymbol{f}^{\mathrm{m}}$ will vanish in the absence of structure fault and shocking.

2.4 Spectral-element method in nutshell

We adopt the full-waveform simulation of acoustic wave propagation in piezoelectric substrates with the spectral-element method, which is a discontinuous Galerkin method with good accuracy, efficiency and parallel implementation. It can solve the wave equation governed by the elastodynamics in the time domain. Here we introduce the basic idea of the method.

Assume the governing system in strong formulation, which is a differential equation, is expressed with a generic mapping operator $\mathcal{L} : L^2(\Omega) \to L^2(\Omega)$:

$$\mathcal{L}u = f, \tag{14}$$

which can also be expressed in a weak formulation, that the inner products are taken with an arbitrary test function v on both sides

$$(\mathcal{L}u, v) = (f, v)\,. \tag{15}$$

If we expand $u \approx \sum_n^N u_n \varphi_n$ and test $v = \varphi_m, m = 1, \ldots, M$, using an orthonormal basis function set $\{\varphi_n\}$, i.e., $(\varphi_n, \varphi_m) = \delta_{nm}$, then Eq. (15) can be expressed in a matrix form:

$$\boldsymbol{AU} = \boldsymbol{F}, \tag{16}$$

where the elements are $a_{mn} = (\mathcal{L}\varphi_n, \varphi_m)$, and $f_m = (f, \varphi_m)$, respectively. Finally, the coefficient array $\boldsymbol{U} = (u_n)$ is obtained as

$$\boldsymbol{U} = \boldsymbol{A} \backslash \boldsymbol{F}. \tag{17}$$

In the interval $[-1, 1]$, the numerical integration of a function $f(x)$ can be approximated by Gaussian-Legendre quadrature

$$\int_{-1}^{1} f(x)dx \approx \sum_{i=1}^{N} w_i f(x_i), \tag{18}$$

in which x_i are the roots of Nth Legendre polynomial $\ell_i^{(N)}(x)$, and the weights w_i are given as

$$w_i = \int_{-1}^{1} \ell_i^{(N)}(x)dx. \tag{19}$$

The orthogonality and completeness of Legendre polynomials can result a diagonal matrix that needs to be inverted, and also bring excellent properties in numerical calculation, thus select them as the basis set

$$\varphi_i \to \ell_i^{(N)}. \tag{20}$$

Time marching is just implemented with a finite difference method.

3 Code instruction

We use the Linux cluster Dardel at KTH as our computing machine, which is a HPE Cray EX supercomputer. The machine is running on SLES 15 SP1 SuSE Linux system, and using the Cray Programming environment and Slurm workload manager to schedule jobs.

Our numerical work is firstly developed in 2D situation. As mentioned that our solver for simulating the acoustic wave propagation in based on the open-source free software SPECFEM, the users first need to a have a copy of the source code of SPECFEM2D, which can be cloned from `github.com` with the following Bash shell script:

```
git clone --recursive --branch devel https://github.com/geodynamics/
    specfem2d.git
```

The code for the project in the simulation of acoustic wave resonators is available to download with the following script:

```
git clone --recursive --branch master https://github.com/yingzi1982/
    acousticWaveFilters2D.git
```

The following script is an illustration about how to make the executables of `xmeshfem2D` and `xspecfem2D`, which are the mesher and the solver, respectively. The compilers need to be decided by the users themselves in their exact computing environment.

```
#!/bin/bash -l
# configure
currentdir=`pwd`
cd ${SPECFEM2D_DIR}
./configure MPI_INC="${CRAY_MPICH2_DIR}/include" --with-mpi MPIFC=ftn MPICC=
    ccc FC=ftn CC=cc CXX=cc

# make
make clean
make xmeshfem2D
make xspecfem2D

# link
cd $currentdir
cp -f ${SPECFEM2D_DIR}/bin/xmeshfem2D ../bin
cp -f ${SPECFEM2D_DIR}/bin/xspecfem2D ../bin
```

The running of the code is simple and straight forward. It has 3 steps: 1. `preprocess.sh`, 2. `specfem.sh`, and 3. `postprocess.sh`. The job may be submitted in whole with a Slurm script with the following example or can run each step individually.

```
#!/bin/bash -l
#SBATCH -A PROJECT_NAME
#SBATCH -p PARTION_NAME
#SBATCH -J JOB_NAME
#SBATCH -t 1:00:00
#SBATCH -N 1

filter_type=SAW
filter_dimension=2D

cd ../bash
./preprocess.sh $filter_type $filter_dimension
./specfem.sh $filter_dimension
./postprocess.sh $filter_type $filter_dimension
```

The script `preprocess.sh` shows bellow is to create mesh model definition, calculate electric field from electrodes, and derivate body force field applied on piezo substrates as the driving sources. The definitions for the sources and receivers are also generated in running the script.

```
#!/bin/bash -l

filter_type=SAW
filter_dimension=2D

```

```
./create_model.sh $filter_type $filter_dimension

./create_converse_piezoelectricity.sh $filter_type $filter_dimension

./create_sources.sh $filter_dimension

./create_stations.sh  $filter_type $filter_dimension
```

The running of SPECFEM has 2 steps: first create meshes with `xmeshfem2D` and then run the solver `xspecfem2D` to simulate wave propagation. The executables can run in serial with single processor `NPROC=1` or in parallel by using multiple cpu-cores.

```
#!/bin/bash -l

NPROC=`grep ^NPROC DATA/Par_file | cut -d = -f 2`

if [ "$NPROC" -eq 1 ]; then
  ./xmeshfem2D
  ./xspecfem2D
else
  srun -n $NPROC ./xmeshfem2D
  srun -n $NPROC ./xspecfem2D
fi
```

After running the solver, the mechanical motions will be recorded as displacement signals by the receivers. The script `postprocess.sh` can convert the mechanical motion to electrical motion and calculate the secondary derivatives such as the charge signals and admittance, etc.

```
#!/bin/bash -l

filter_type=SAW
filter_dimension=2D

./process_traces.sh $filter_type $filter_dimension
```

4 Numerical examples

In this part, we present our numerical simulation results with the simple models to validate our algorithm and code. We investigate the surface acoustic wave resonator as the example.The surface acoustic wave devices are based on the transduction of the waves propagate along the free surface, mainly in the form of Rayleigh waves, and have wide application in telecommunication, environmental sensing and microfluidics, etc. The devices are accomplished by the use of piezoelectric materials as substrates and interdigital transducers as electrodes to convert acoustic waves to electrical signals and vice versa.

We take Lithium Niobate ($LiNbO_3$) as the piezoelectric substrate in our numerical model. The material's physical parameters of the density, dielectric constant, piezoelectric constant

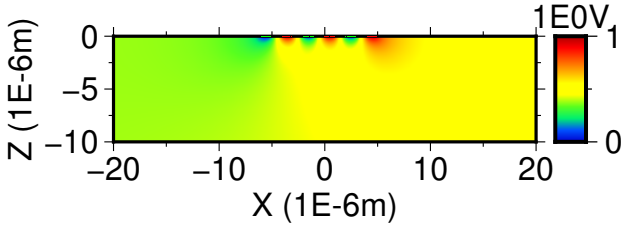

Figure 3: Electric potential scalar field.

and elastic constant are given in Eqs. (21)-(24), respectively.

$$\rho = 4640(\mathrm{kg/m^3}), \tag{21}$$

$$\boldsymbol{\epsilon} = \begin{pmatrix} 85.2 & 0 & 0 \\ 0 & 85.2 & 0 \\ 0 & 0 & 28.7 \end{pmatrix} \times 8.55 \times 10^{-12}(\mathrm{F/m}), \tag{22}$$

$$\boldsymbol{e} = \begin{pmatrix} 0 & 0 & 0 & 0 & 3.83 & -2.37 \\ -2.37 & 2.37 & 0 & 3.83 & 0 & 0 \\ 0.23 & 0.23 & 1.3 & 0 & 0 & 0 \end{pmatrix} (\mathrm{C/m^2}), \tag{23}$$

$$\boldsymbol{c} = \begin{pmatrix} 2.030 & 0.573 & 0.752 & 0.085 & 0 & 0 \\ & 2.030 & 0.752 & -0.085 & 0 & 0 \\ & & 2.424 & 0 & 0 & 0 \\ & & & 0.595 & 0 & 0 \\ & & & & 0.595 & 0.085 \\ & & & & & 0.728 \end{pmatrix} \times 10^{11}(\mathrm{Pa}). \tag{24}$$

Its parameters are general direction dependent, that different crystal cutting orientation will result different performance. Here we don't apply the crystal coordinate rotation, which can be easily transformed at a particular Euler angles in the user's definition.

In the 2D models we just adopt the X-Z plane as the simulation domain, that the Rayleigh waves propagate in the X-direction. From our model setting, the P-wave velocity in the X-direction can be derived as $v_P = \sqrt{c_{11}/\rho} = 6607$ m/s, and the S-wave velocity in the X-direction with Z-direction polarisation is $v_S = \sqrt{c_{55}/\rho} = 3577$ m/s. The analytical solution for the Rayleigh wave velocity, especially in an anisotropic solid, is general complicated, but it may be approximated as[9]:

$$v_R = \frac{0.862 + 1.14\nu}{1 + \nu} v_S, \tag{25}$$

where the Poisson ratio is $\nu = 0.25$ for $LiNbO_3$, that the Rayleigh wave velocity in the X-direction is about $v_R = 3282$ m/s in our model setting.

A simple model with a small number, 3 pairs for example, interdigital transducers is first investigated. The positive and negative electrodes with the same width of 1μm are deployed on the top surface, the metallisation rate is set as 50% that the gaps between the electrodes is also 1μm. For the surface acoustic wave devices, the horizontal range is extended and normally appended with an acoustical absorbing material or Bragg reflectors, and the lower is a half-space that the reflections from the left and right sides and the bottom should be eliminated.

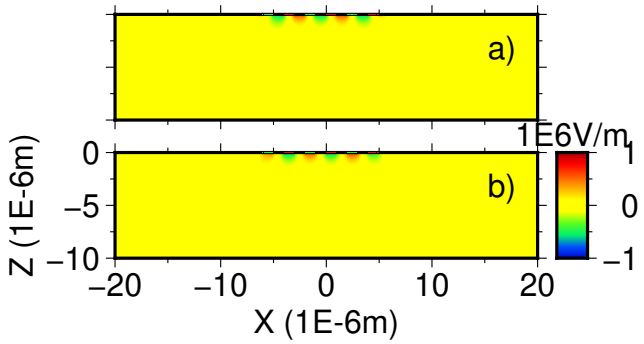

Figure 4: Electric vector field. a) X-component; b) Z-component.

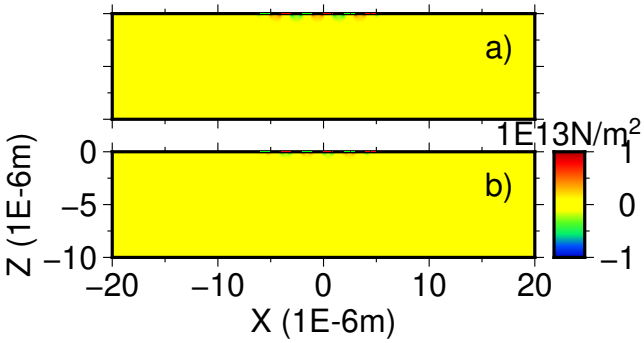

Figure 5: Body force vector field. a) X-component; b) Z-component.

So these 3 interfaces are set as absorbing boundaries with the perfectly matched layers, while the top interface is in a free boundary condition.

When an unit amplitude voltage is applied on the positive electrode while the negative electrode is grounded, Figure 3 illustrates the electric potential field caused by the applied voltages on the electrodes. Furthermore, we can derivate the electric field by taken the gradient of the electric potential field, and the horizontal and vertical components of the vector field are shown in Figure 4.

Upon the application of electric field, the stress field is generated through the converse piezoelectric effect. The stress is a second order tensor and alternatively we can express such internal force effect with the body force, which is the divergence of stress. From the plotting of body force field in Figure 5, we can see that the opposite forces periodically act with a spacing of the length of finger pitch, that is $L_P = 2\mu$m in our setting, so we should expect the superposition of coherent waves at the central wavelength of $\lambda_0 = 2L_p = 4\mu$m, that the resonant frequency will be estimated at $f_0 = v_S/\lambda_0 \approx 0.821$ GHz in our model setting.

When a voltage excitation signal is applied on the two electrode terminals, the waves will be generated. Here we adopt a 1GHz central frequency Ricker wavelet as the input signal. In Figure 6 we show the animation of the generation and propagation of waves in our model. We can see that a small portion of body waves are generated but the main wave energy is in the form of Rayleigh waves, which propagate in left and right directions and each train has 3 carriages in this case. The waves vanish at the numerical absorbing boundaries.

Furthermore, we can also illustrate the evolution of waves both in the time and spatial

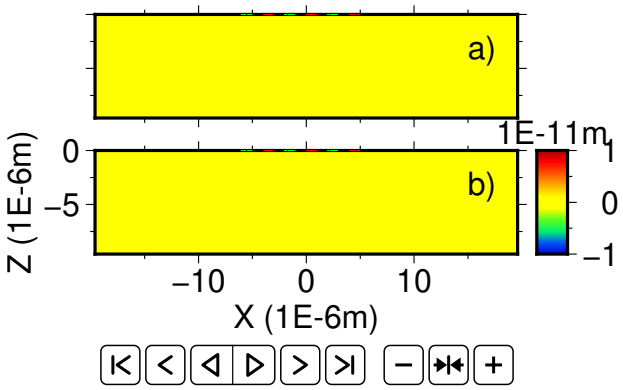

Figure 6: Displacement snapshots. a) X-component; b) Z-component.(View animation with Adobe Acrobat Reader.)

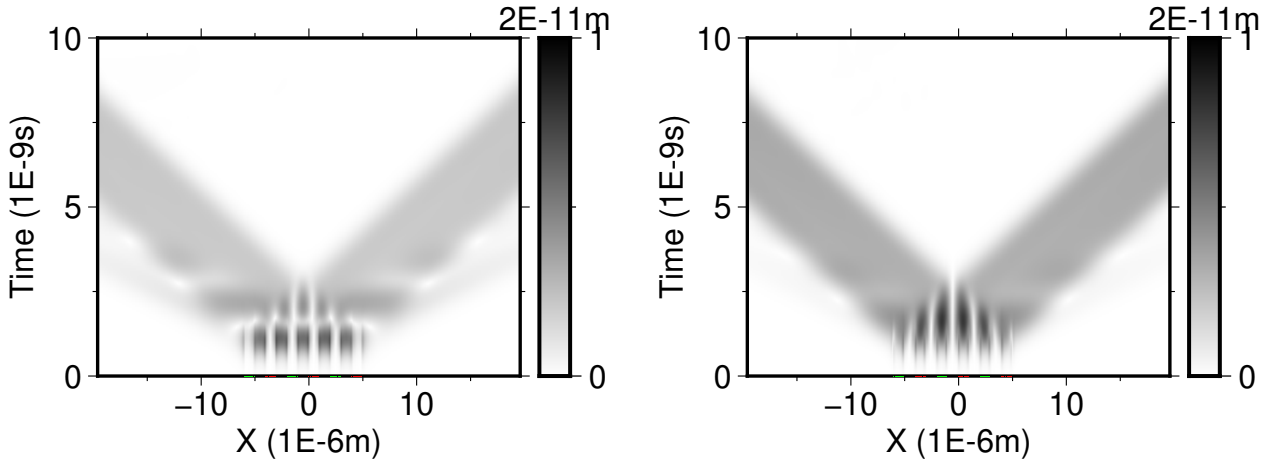

(a) X-component

(b) Z-component

Figure 7: Tempo-spatial structure of displacement field on the top free surface.

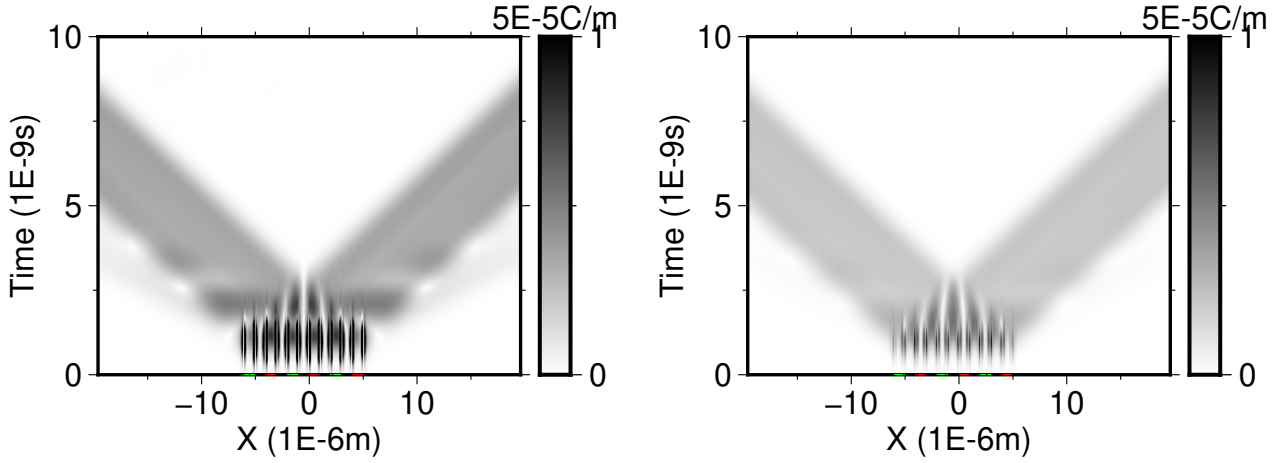

(a) X-component (b) Z-component

Figure 8: Tempo-spatial structure of electric displacement field on the top free surface.

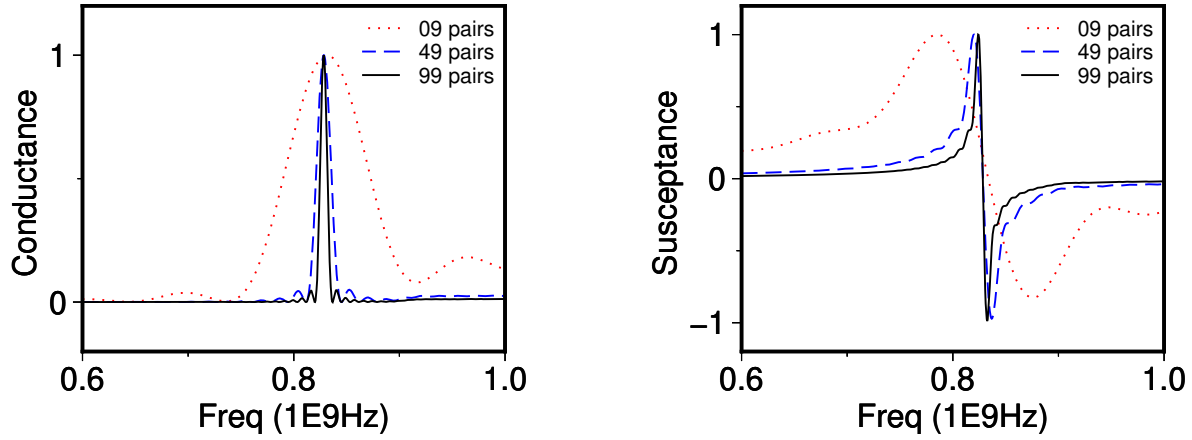

(a) Real component (b) Imagery component

Figure 9: Comparison of the admittance spectra of the surface acoustic wave filters with 9, 49 and 99 pairs of fingers.

domains, as shown in Figure 7 for the displacement signal traces on the top surface against the time varying.

The deformation of piezoelectric material will result charge accumulation on the surface according to the direct piezoelectric effect. In Figure 8 the time evolution of electric displacement on the top surface is plotted. The total charge on electrode is summed over the surface of electrodes and the current is generated when the charge is in movement due to the amount change.

The admittance of a filter, a reciprocal of impedance, is defined as the ratio of the measured electric current over the applied voltage:

$$Y(\omega) = \frac{I(\omega)}{V(\omega)} = G(\omega) + iB(\omega), \tag{26}$$

which characterizes the easiness of an acoustic wave filter to allow a current to flow. The real

and imaginary components of admittance spectra are the conductance and the susceptance, respectively, both are measured in the unit of Siemens.

We simulate the surface acoustic wave filters in the 3 cases with 9, 49 and 99 pairs of electrode fingers, and calculate the real and imaginary components of the admittance spectra, which are plotted with the normalised amplitudes in Figure 9. We can see that the central resonance frequency is at the peak of conductance but at the zero of susceptance, which is measured at 0.828 GHz. It is very close to the previous estimation at 0.821 GHz, and the bias is mainly from the rough estimation of the Rayleigh wave velocity. When the pair number increases, the central resonance frequency is unchanged but the band becomes narrowing, as shown in the conductance and susceptance plotting. In the case of 99 pair fingers in our model setting, the series and parallel resonance frequencies are measured at 0.824 GHz and 0.833 GHz, respectively.

5 Conclusions and Future Work

In summary of the progress in this project, we have mainly:

- Systematically organised the fully theories govern the acoustic wave resonators;
- Developed the prototyping code for the 2D numerical simulator;
- Performed the numerical simulations of surface acoustic wave resonators and verified the practicality of our algorithm, method and code;
- Revealed the intrinsic mechanism of acoustic wave resonators through the full-waveform simulation.

We will further develop the code for a full 3D simulator, and the final goal is to incorporate all the code into the SPECFEM packages and release a stand-alone executables with simple I/O interfaces. The modelling of other types filters like bulk acoustic wave filters, or more featured structures like grating and reflector, is mainly about different mesh building, which will just follow the similar procedures with the same simulator.

References

[1] Ken-ya Hashimoto and Ken-Ya Hashimoto. *Surface acoustic wave devices in telecommunications*, volume 116. Springer, 2000.

[2] Dimitri Komatitsch and Jean-Pierre Vilotte. The spectral element method: an efficient tool to simulate the seismic response of 2d and 3d geological structures. *Bulletin of the Seismological Society of America*, 88(2):368–392, 1998.

[3] Dimitri Komatitsch and Jeroen Tromp. Introduction to the spectral element method for three-dimensional seismic wave propagation. *Geophysical Journal International*, 139(3):806–822, 1999.

[4] Jeroen Tromp, Dimitri Komatitsch, and Qinya Liu. Spectral-element and adjoint methods in seismology. *Communications in Computational Physics*, 3(1):1–32, 2008.

[5] Daniel Peter, Dimitri Komatitsch, Yang Luo, Roland Martin, Nicolas Le Goff, Emanuele Casarotti, Pieyre Le Loher, Federica Magnoni, Qinya Liu, Céline Blitz, et al. Forward and adjoint simulations of seismic wave propagation on fully unstructured hexahedral meshes. *Geophysical Journal International*, 186(2):721–739, 2011.

[6] Christina Morency and Jeroen Tromp. Spectral-element simulations of wave propagation in porous media. *Geophysical Journal International*, 175(1):301–345, 2008.

[7] Specfem2d user manual.

[8] Bertram Alexander Auld. *Acoustic fields and waves in solids*. 1973.

[9] LB Freund. *Dynamic fracture mechanics, Cambridge University Press*. 1990.